Supplementary Information

1. Cyclic voltammetry

Was done as described in the main article. As control experiments the CVs of the CcO immobilized with the his-tag attached to subunit II (Fig. 1A, main article) taken after activation in an anaerobic (red line, right hand y-axis) and aerobic (black line, left hand y-axis) solution recorded in the same potential window are added. The increase of the height of the electron transfer peak and the disappearance of the proton peak can be clearly seen, as is the disappearance of peaks in the positive range of potentials. In addition a CV of the CcO immobilized with the his-tag attached to subunit I (Fig. 1B, main article) (red line with red squares, right hand y-axis) was measured. No peaks are recorded in this orientation.

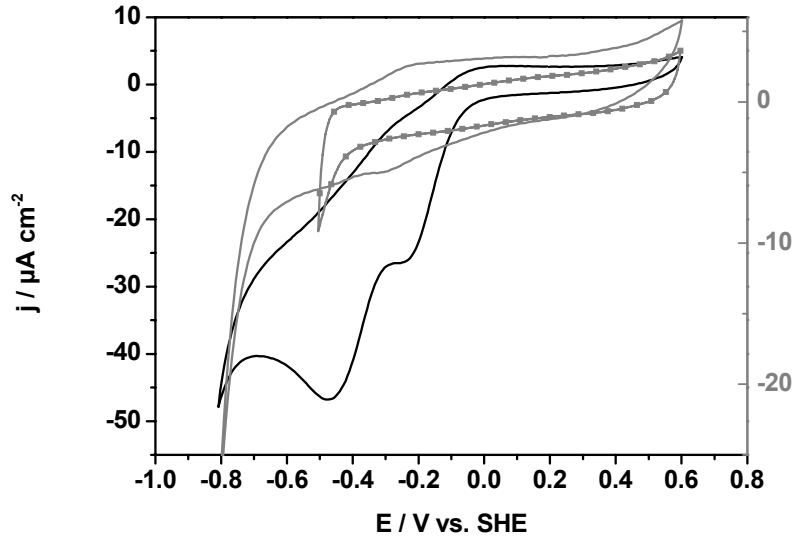

Fig. 1. CVs of the CcO on TSG immobilized with the His-tag attached to subunit II, under anaerobic (red, right hand y-axis) and aerobic (black, left hand y-axis) conditions, both in the activated state, scan rate 50 mV/s, CV of the CcO immobilized with the his-tag attached to subunit I (red line red squares, right hand y-axis)

In order to take into account the difference in roughness between the smooth TSG and the two-layer gold surface, a CV of the CcO in the activated state under anaerobic conditions (corresponding to Fig. 2C) were recorded on the two-layer gold surface. The result is shown in Fig. 2. The two CVs are very well comparable so that ET does not seem to be largely affected by the roughness.

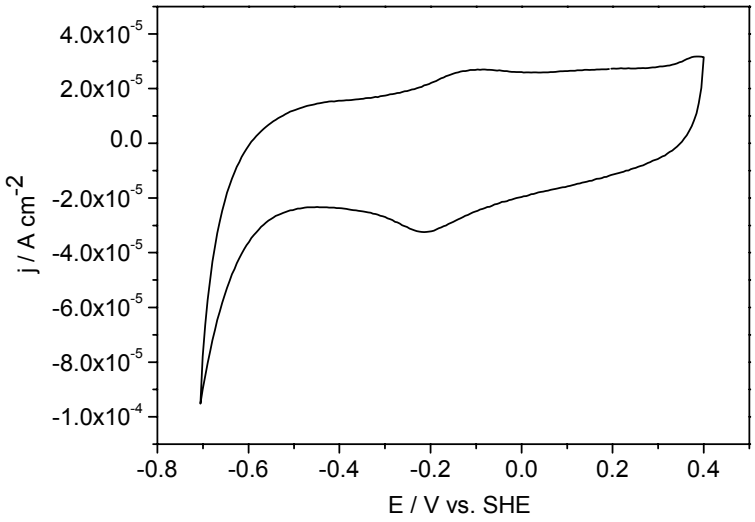

Fig. 2. CV of the CcO immobilized on the two-layer gold surface with the His-tag attached to subunit II, under anaerobic conditions, in the activated state, scan rate 50 mV/s,

2. Spectro-electrochemical measurements

Spectra were evaluated using the OPUS software (Bruker Optics). After base line correction, spectra were corrected with respect to the bending vibration of water molecules with a band at 1643cm^{-1}. In order to be able to do the correction effectively, it was useful to keep the temperature of the spectro-electrochemical cell constant at 27° C using a thermostat. After correction of the water bands, spectra were deconvoluted also using the OPUS software. Examples of baseline corrected and deconvoluted spectra are given in Supp. Fig. 2A for the activated and 2B for the deactivated CcO. Bands between 1300 and 2800 cm^{-1} were described in the main article. The band at 2110cm^{-1} is due to the valence vibration of phospholipid molecules, which strongly depends on the electric field applied across the protein/lipid layer.

The spectrum of the CcO in the orientation given in Fig. 1A of the main article was taken for comparison purposes before any potential was applied. The band at 1641 cm^{-1} is characteristic for the amide the I C=O stretching vibration of β-sheets, which are nearer to the surface of the ATR crystal than the α-helices. The band at 1532 cm^{-1} indicates the amide II C-N stretching and N-H bending vibrations, respectively. The band at 1284 cm^{-1} is due to the amide III C-N and N-H vibrations. Bands at 1441 and 1382 cm^{-1} are characteristic for the COOH groups of the NTA residue. Spectra are recorded every two minutes (from bottom to top).

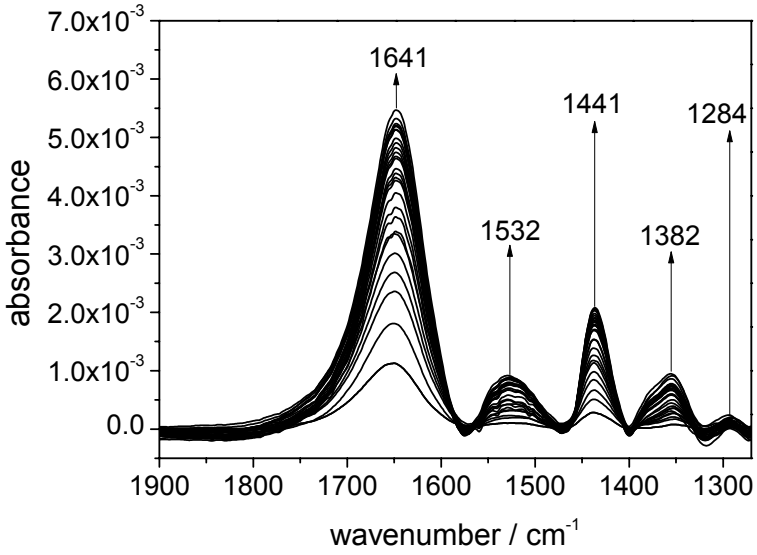

Fig. 3. Spectra of the CcO in the orientation with Cu A directed toward the electrode (His-tag attached to subunit II, Fig. 1A main article) as a function of time during immobilization, from bottom to top, without any potential applied

The spectrum of the CcO in the orientation given in Fig. 1B of the main article was taken for comparison purposes before any potential was applied. The bands at 1657 cm^{-1} is characteristic for the amide the I C=O stretching vibration of α-helices, which in this orientation are nearer to the surface than the β-sheets. The band at 1513 cm^{-1} indicates the amide II C-N stretching and N-H bending vibrations. The band at 1282 cm^{-1} is due to the amide III C-N and N-H vibrations. Bands at 1441 and 1384 cm^{-1} are characteristic for the COOH groups of the NTA residue. Spectra are recorded every two minutes (from bottom to top).

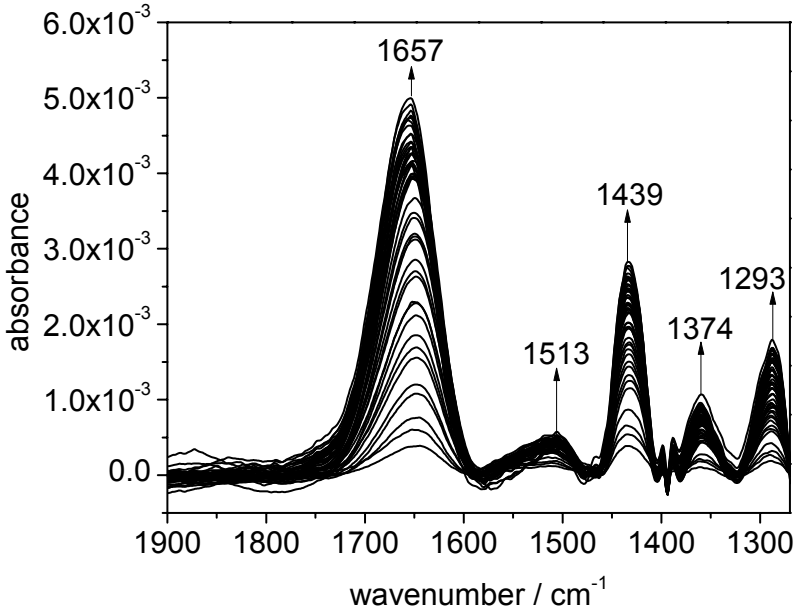

Fig. 4. Spectra of the CcO in the orientation with Cu A directed away from the electrode (His-tag attached to subunit I, Fig. 1B main article) as a function of time during immobilization, from bottom to top, without any potential applied

3. Potentiometric titration of CcO by surface-enhanced ATR-IR-Spectroscopy

Difference spectra reduced-minus-fully oxidized for activated (A) and non-activated (B) CcO immobileized via His-tag on subunit II (cf Fig. 1A). Potential applied was 900 mV vs. SHE for the fully oxidized state and varied from 500 mV to – 700 mV in 100 mV steps for reduced states (bottom to top). No mediators added. The titration had to be completed within 30 min. Otherwise the protein relaxed back to the non-activated state.

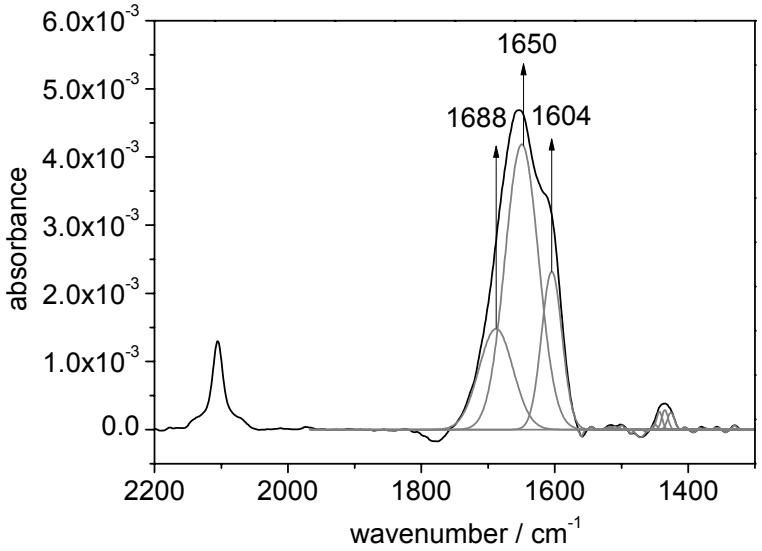

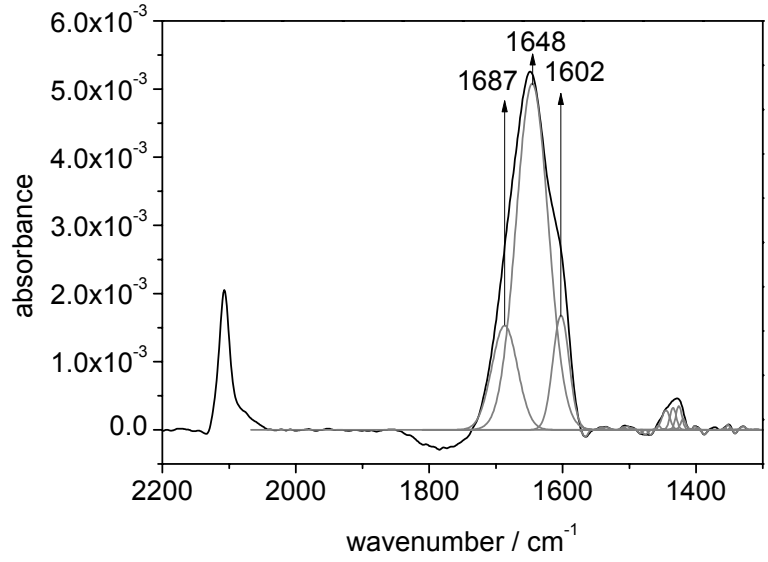

Fig. 5. Examples of deconvoluted spectra of the CcO in the activated (A) and non-activated state (B) recorded at -800 mV

For the potentiometric titration in the presence of the mediators CcO from *Paracoccus denitrificans* genetically engineered with the His-tag on SU I was immobilized and reconstituted into a lipid membrane as described in ref. 15, 16, 22 of the main article. Titration was done according to refs. 7, 9 of the main article. Mediators used are given in Table 1. They are added to the buffer solution at a concentration of 40 µmol/l

Table 1. List of the mediators with molecular structures and redox potentials

		E_m [mV] vs SHE
methyl viologen	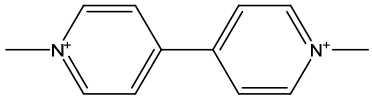	-444
benzyl viologen	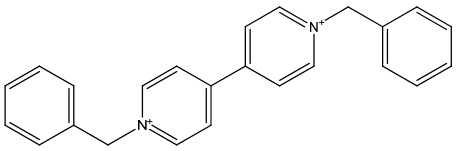	-360
anthraquinone-2-sulfonate	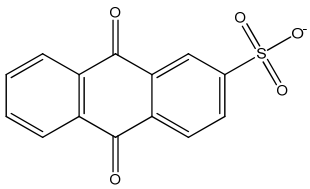	-225
2-hydroxy-1,4-naphthoquinone	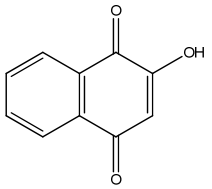	-125
menadione (2-methyl-1,4-naphthoquinone)	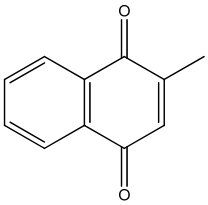	-12

trimethylhydroquinone	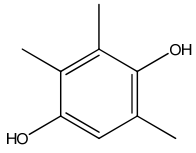	100
1,2-naphthoquinone	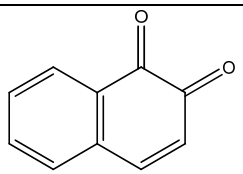	145
ruthenium hexamine chloride	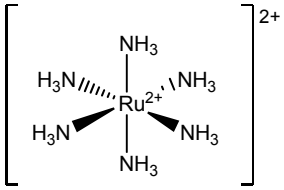	200
2,6-dichlorophenolindophenol	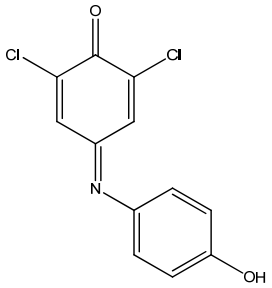	217
tetramethylparaphenylen-diamine	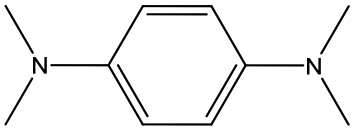	270
1-1'-dimethylferrocene	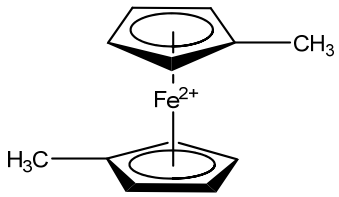	341
dimethylparaphenylen-diamine		371
ferricyanide	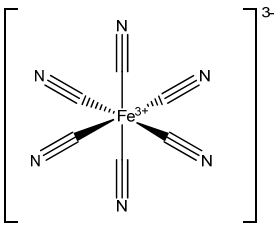	424

1,1'-dicarboxylferrocene	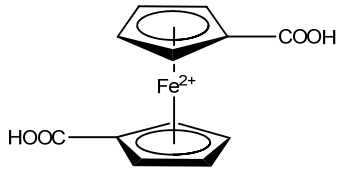	644

4. Assessment of unspecific absorption and its contribution to the sigmoid function

The assessment of the contribution due to unspecific absorption would require an enzyme with inactive ET to Cu_A but otherwise identical to the protein under study, which is not feasible. The enzyme that comes closest to this requirement is CcO with the His-tag attached to SU I immobilized on the electrode. Since Cu_A is pointing away from the electrode direct ET does not occur (see Fig. 1 and Fig. 1 of the main article). The result of a titration with this preparation in the direction of negative potentials, performed and analyzed as described above, is shown in Fig. 6 for the band at 1605 cm^{-1}. Although these data cannot be directly compared with the data in Fig. 4 of the main article primarily because of the reverse orientation of the CcO, but also because of different surface coverage (i.e. mole number of protein per unit area) and different sources (*P. denitrificans* versus *R. sphaeroides*) it is nevertheless evident that unspecific absorbance changes may be substantial. In the present case they show a monotonously curved dependence on potential, but other dependences ranging from linear see ref 29 of the main article to more complex functions were also found. We have tentatively assumed a sigmoid dependence according to

$$A = \frac{\Delta A_{\mathrm{us}}}{1 + \exp[(E - E_{\mathrm{us}})/\varphi_{\mathrm{us}}]} + A_{0,\mathrm{us}} \qquad (1)$$

and could successfully fit it to the data in Fig. 6.

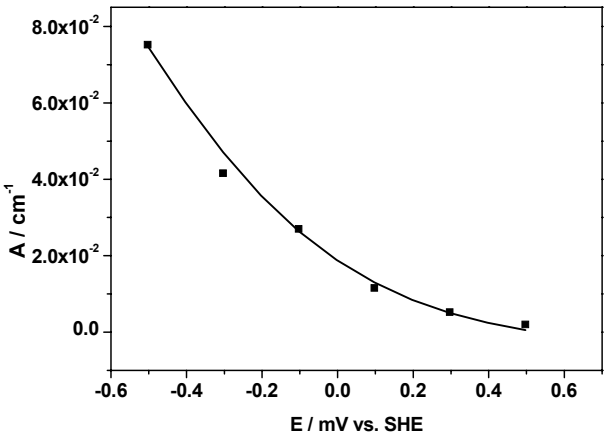

Fig. 6. Dependence of band area A on applied potential E in the absence of ET. Reductive titration of CcO from *P. denitrificans* immobilized via His-tag on subunit I. No mediators added. Band at wavenumber 1605 cm^{-1}. The curve represents eq. 2 fitted to the data, parameter values: $E_{\mathrm{us}} = -625 \pm 528$ mV, $\varphi_{\mathrm{us}} = 311 \pm 142$ mV, $\Delta A_{\mathrm{us}} = 0.20 \pm 0.20$ cm^{-1}, $A_{0,\mathrm{us}} = -0.005 \pm 0.007$ cm^{-1}. Note that the uncertainty of the parameter values is large because the experimental data cover only the "tail" of a sigmoid curve.

In view of this result we have further assumed that eq. 1 can also be applied to the redox titrations presented in Fig. 5 (with different values for parameters though) and hence have attempted to analyze these data by means of a relation comprising two terms, the first one accounting for the redox-related (rr) and the second one for the unspecific (us) contribution (cf. eqs.1 and 2),

$$A = \frac{s\Delta A_{\mathrm{rr}}}{1+\exp[s(E-E_{\mathrm{rr}})/\varphi_{\mathrm{rr}}]} + \frac{s\Delta A_{\mathrm{us}}}{1+\exp[s(E-E_{\mathrm{us}})/\varphi_{\mathrm{us}}]} \qquad (2)$$

$$\text{with } s = \begin{cases} +1 \text{ for red. titr} \\ -1 \text{ for ox. titr} \end{cases}$$

Since this analysis requires a closer spacing of potential values than that of the experimental data we have calculated data by means of eq. 1 (without the correction term A_0) using the parameter values listed in Table 2. When fitting eq. 2 to these data we have found that the separation of redox-related and unspecific absorbance changes is basically feasible, however not all parameters can be fitted simultaneously but two of them have to be fixed.

If the redox-related contribution behaves ideally it can be described by the Nernst equation, i.e. $\varphi_{\mathrm{rr}} = RT/F \approx 26$ mV. Keeping this parameter together with either E_{us} or φ_{us} fixed and analyzing the data for reductive and oxidative titration separately revealed that the deviation of φ from the theoretical value (see Table 2 main article) can be fully accounted for by φ_{us}. But the two E_{rr} values came out so differently that a common value could not be found, which indicates that a hysteresis for the redox-related contribution does exist. At present it is not possible to attribute the hysteresis to one of the processes, i.e. to decide whether the redox states do not reach equilibrium and/or the conformational states do not equilibrate with the redox states. But an illustrative example of a possible hysteresis loop can be obtained as follows. The band areas for the reductive titration are scaled such that they cover the same range as those for the oxidative titration, which also may account for a possible difference in surface coverage in the two preparations. The same and fixed values for ΔA_{rr} as well as for φ_{rr} ($\neq RT/F$) can then be used when fitting eq. 2 to the data of the two titrations. The result is presented in Fig. 7 of the main article for the band at 1605 cm^{-1} of activated CcO (cf. Fig. 5D).
Parameter values: fixed $\Delta A_{\mathrm{rr}} = 0.0033$ cm^{-1}, $\varphi_{\mathrm{rr}} = 20$ mV; fitted E_{rr} / mV = −187 ± 2 and −26 ± 3, E_{us} / mV = −209 ± 9 and −47 ± 12, φ_{us} / mV = 81 ± 5 and 103 ± 8, $\Delta A_{\mathrm{us}} \times 10^3$ cm = 2.24 ± 0.05 and 2.21 ± 0.05 for reductive and oxidative titration, respectively.